American Mineralogist, Volume 97, pages 1891–1897, 2012

A single-crystal neutron diffraction study of hambergite, $Be_2BO_3(OH,F)$

G. Diego Gatta,[1,2,*] Garry J. McIntyre,[3] Geoffrey Bromiley,[4] Alessandro Guastoni,[5] and Fabrizio Nestola[5]

[1]Dipartimento di Scienze della Terra, Università degli Studi di Milano, Via Botticelli 23, I-20133 Milano, Italy
[2]CNR-Istituto per la Dinamica dei Processi Ambientali, Milano, Italy
[3]Australian Nuclear Science and Technology Organisation, Locked Bag 2001, Kirrawee DC, New South Wales 2232, Australia
[4]School of GeoSciences, The University of Edinburgh, The King's Buildings, West Main Road, Edinburgh EH9 3JW, U.K.
[5]Dipartimento di Geoscienze, Università degli Studi di Padova, Via Gradenigo 6, I-35131 Padova, Italy

Abstract

The crystal chemistry and crystal structure of hambergite from the Anjanabonoina mine, Madagascar [$Be_2BO_3(OH)_{0.96}F_{0.04}$, $Z = 8$, $a = 9.762(2)$, $b = 12.201(2)$, $c = 4.430(1)$ Å, $V = 527.6(2)$ Å^3, space group *Pbca*], were reinvestigated by means of electron microprobe analysis in wavelength-dispersive mode, secondary-ion mass spectrometry, single-crystal X-ray and neutron Laue diffraction. Chemical analyses show only a small amount of F (0.7–0.8 wt%, approximately 0.04 atoms per formula unit) substituting OH and no other substituent at a significant level. An anisotropic neutron structural refinement has been performed with final agreement index $R_1 = 0.0504$ for 76 refined parameters and 1430 unique reflections with $F_o > 4\sigma(F_o)$. The geometry of the hydroxyl group and hydrogen bonding in hambergite is now well defined: (1) only one independent H site was located and the O4-H distance, corrected for "riding motion," is ~0.9929 Å; (2) only one hydrogen bond appears to be energetically favorable, with a symmetry-related O4 as *acceptor* and with O4···O4 = 2.904(1) Å, H···O4 = 1.983(1) Å, and O4-H···O4 = 157.5(1)°. In other words, O4 sites act both as *donor* and as *acceptor* of the hydrogen bond, with a zigzag chain of H-bonds along [001]. The hydrogen-bonding scheme in hambergite found in this study is consistent with the pleochroic scheme of the infrared spectra previously reported, with two intensive modes ascribable to stretching vibrations of the hydroxyl group, at 3415 and 3520 cm^{-1}, respectively. The two modes suggest at least two distinct hydrogen-bonding environments, ascribable to the presence of oxygen and fluorine at the *acceptor* site.

Keywords: Hambergite, crystal chemistry, electron microprobe analysis in wavelength-dispersive mode, secondary-ion mass spectrometry, neutron Laue diffraction, hydrogen bonding

Introduction

Hambergite, ideal composition: $Be_2BO_3(OH,F)$, is an uncommon accessory mineral originally described from an alkaline syenitic pegmatite from Norway by Brögger (1890). However, the majority of hambergite occurrences are in complex Li-rich granitic pegmatites of the elbaite or transitional elbaite-lepidolite subtypes (e.g., Switzer et al. 1965; Novák et al. 1998 and references therein).

The crystal chemistry of hambergite is somewhat unique in nature ($B_2O_5 \approx 36$ wt%, BeO ≈ 54 wt%, $H_2O \approx 8$ wt%, F ≈ 2 wt%). Its crystal structure was solved by Zachariasen (1931) in the space group *Pbca* with $a \approx 9.8$, $b \approx 12.2$, and $c \approx 4.4$ Å. The experimental limitations at that time allowed the author to propose a general structure model only. However, for the first time it was found that the borate group exists as an almost perfect oxygen triangle with the boron atom at its center. These experimental findings opened a new scenario in solid-state chemistry, leading Zachariasen (1934), for example, to solve the crystal structure of boric acid (H_3BO_3, triclinic polymorph), in which an identifiable BO_3 triangle also exists, this time with a hydrogen bonded to each oxygen, and so suggesting that the structure is better written as $B(OH)_3$. Later, the crystal structure of hambergite was reinvestigated by Zachariasen et al. (1963) and Burns et al. (1995). The structure of this mineral contains two different building-block units: $BeO_3(OH)$ tetrahedra and BO_3 triangles. Each non-hydroxyl oxygen atom of the $BeO_3(OH)$ tetrahedra is shared with another $BeO_3(OH)$ unit and a BO_3 triangle (Fig. 1). The OH group is shared between two $BeO_3(OH)$ tetrahedra and the BO_3 triangles lie in a plane parallel to [001] (Fig. 1). Such an inter-polyhedral connection leads to a framework-like structure, as shown in Figure 1, with distorted channels running along [001].

Vergnoux and Ginouvès (1955) reported polarized infrared spectra for hambergite, which indicate a bond angle for hydrogen (i.e., O-H···O) considerably smaller than 180°. Switzer et al. (1965) reported the crystal chemistry of hambergite crystals from several localities, and found that considerable F (up to 6 wt%, which corresponds to ~0.3 atoms per formula unit, apfu) can replace OH in the structure. A comparative study of the crystal structure of hambergites from several localities and with different F content by Burns et al. (1995) showed that the F/OH substitution causes a significant change of the unit-cell dimensions.

All previous investigations of the crystal structure and crystal chemistry of hambergite (e.g., Zachariasen 1931; Vergnoux and

* E-mail: diego.gatta@unimi.it

0003-004X/12/1112–1891$05.00/DOI: http://dx.doi.org/10.2138/am.2012.4232

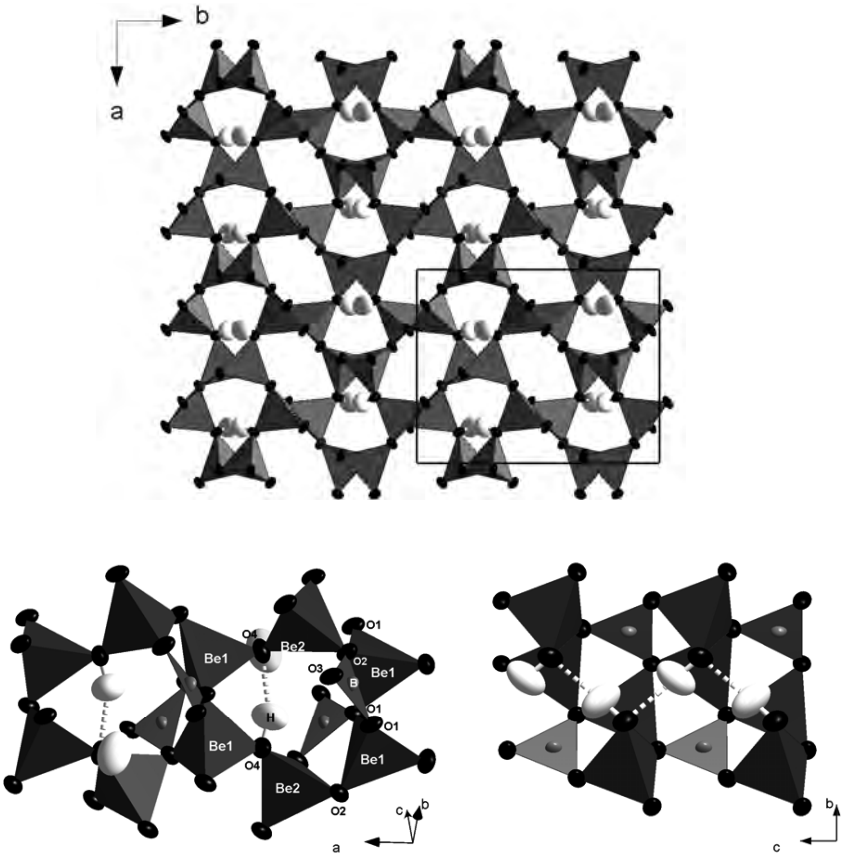

Figure 1. The crystal structure of hambergite based on the structure refinement of this study at 298 K. The H-bonding scheme is shown. Displacement ellipsoid probability factor: 99%.

Ginouvès 1955; Zachariasen et al. 1963; Burns et al. 1995) suggest that hydrogen bonds play an important role in stabilizing the framework structure, but clarification of this role is obscured by difficulties in determining proton positions. All structure refinements of hambergite have been performed on the basis of X-ray diffraction data, resulting in a poorly defined picture of the configuration of the O-H groups (e.g., with O-H distances ranging between 0.69 and 0.84 Å; Burns et al. 1995) and of the H-bonding. In light of this, the aim of the present study is to re-investigate the crystal structure and crystal chemistry of a natural hambergite at ambient conditions by means of electron microprobe analysis in wavelength-dispersive mode, secondary-ion mass spectrometry, and single-crystal X-ray and neutron Laue diffraction, to provide:

(1) reliable location of the proton site(s) and the real topological configuration of the OH group(s), for a full description of the atomic relationship via the H bond;

(2) anisotropic displacement parameters of all the atomic sites, H included;

(3) any potential F/OH ordering.

The scattering lengths of Be (7.79 fm), B (5.30 fm), O (5.805 fm), F (5.654 fm), and H (–3.7409 fm) (Sears 1986) suggest that single-crystal neutron diffraction provides the only experimental technique that will allow us to answer the open questions about the crystal structure/chemistry of hambergite. This study is the latest in a series of single-crystal neutron diffraction experiments that we have recently devoted to B/Be-bearing minerals (Gatta et al. 2006, 2008, 2010).

Sample description and mineralogy

The hambergite used for this multi-methodological study is a fragment of a large, colorless, transparent, tabular crystal, measuring $5 \times 3 \times 1$ cm^3, belonging to the collection of the Museum of Mineralogy of The University of Padova (ref. code: MMP M6930). The crystal was collected at the Anjanabonoina mine, located in the central highlands of Madagascar, approximately 55 km west of Antsirabè. Hambergite is a typically rare accessory mineral of miarolitic pegmatites. This region of Madagascar hosts numerous gem-bearing pegmatites, famous for producing gem-quality tourmaline, morganite, kunzite, and other minerals for over a century. Many of the gem-bearing pegmatites in central Madagascar, including Anjanabonoina, are hosted by rocks of the Itremo Group, in a tectonic unit known as the "Itremo thrust sheet." The Itremo Group is characterized by a lower unit of gneiss and an upper unit of quartzites, schists, and marbles (Fernandez et al. 2001). Anjanabonoina pegmatite is hosted within marbles and has been intensively exploited for gem-quality tourmaline, liddicoatite, and elbaite. In these pegmatites,

hambergite occurs in gem-bearing "pockets" or cavities, which are rare but up to several meters in length. These pockets are surrounded by kaolin clay and contain assemblages of quartz, microcline feldspar (amazonite), albite feldspar (cleavelandite), dravite-elbaite-liddicoatite tourmaline, spodumene (kunzite), native bismuth, spessartine, beryl (morganite), hambergite, danburite, phenakite, and scapolite (Pezzotta 1996, 2001). Large areas of the Anjanabonoina pegmatite are severely kaolinized by the activity of late-stage hydrothermal fluids. The rocks are also deeply weathered to depths exceeding 20 m, particularly in the southern portion of the mining area where extensive eluvial deposits were worked (Dirlam et al. 2002). The Anajanabonoina pegmatite shows a geochemical "mixed" lithium, caesium, tantalum (LCT) and niobium, yttrium, fluorine (NYF) signature, following Černý and Ercit's (2005) classification, where high-geochemically evolved core zones are enriched with LCT minerals (e.g., elbaite-liddicoatite, Li-rich micas, spodumene, hambergite, pink-beryl) and other portions where NYF minerals are abundant (like microcline, pyrochlore, monazite, and allanite) (De Vito et al. 2006).

Experimental methods

Chemical analysis

The chemical composition of our hambergite sample from Anjanabonoina was investigated by electron microprobe analysis in wavelength-dispersive mode (EMPA-WDS) and secondary-ion mass spectrometry (SIMS).

The EMPA-WDS investigation was aimed mainly at detecting the presence of F and other potential substituents for Be (e.g., Al, Si, Fe^{3+}, Switzer et al. 1965). Electron microprobe analysis was performed on a polished sample using a JEOL JXA-8200 microprobe in wavelength-dispersive mode. The system was operated using an accelerating voltage of 15 kV, a beam current of 15 nA and beam diameter of 5 μm, and a counting time of 30 s on the peaks and 10 s on the background. A series of natural minerals were used as standards (F-apatite for F, anorthite for Al and Si, fayalite for Fe). However, only F was detected above the detection limit. The data corrected for matrix effects (using the ΦρZ method as implemented in the JEOL suite of programs) gave: 0.81(8) wt% F (12 data points).

SIMS measurements were performed using a Cameca IMS4f ion microprobe at the NERC IMF (University of Edinburgh), with a 5 nA ^{16}O-primary beam of 15 keV impact energy for positive secondary ions and 6 keV for negative secondary ions. Secondary ions were produced at 4.5 keV in both negative and positive mode. A liquid-nitrogen cold trap was used to reduce volatile-element presence. Measurements were made using single-ion counting and entrance slits closed to give <1 million cps. No fractionation was expected under differing entrance-slit conditions. Measurements were made under various energies to determine possible effects of instrumental parameters on Be/B sample yield, to verify the accuracy of the analytical results. No significant differences were observed between Be/B ion yields measured at different energies, i.e., the energy distributions of B and Be were similar as both positive and negative ions.

Negative secondary ions. SRM610 (a trace-element glass) was used as a standard, and gave negative-ion yields for Be/B of 0.236. Measurements were made using offsets of 0, 50, and 75 eV. The hambergite sample gave a Be/B ratio of 1.93 ± 0.02 (1σ based on a mean of 5 measurements at each offset). H_2O and F contents of the sample were calculated on the basis of counts rates at a 50 eV offset using a rhyolitic glass standard. The hambergite sample was determined to contain 14 wt% OH and 0.7 wt% F, which correspond to 0.957 and 0.043 apfu, respectively.

Positive secondary ions. Be/B positive-ion yields for the same SRM610 glass standard were 2.40. Ion yields for Be/B based on Be/Ca ratios determined in a hurlbutite (Ca-Be-phosphate) and B/Ca ratios in a borosilicate standard were 2.34. On the basis of this calibration and using offsets of 0 and 75 eV, the Be/B ratio measured in the hambergite sample was 1.96 ± 0.01 (1σ based on a mean of 7 measurements at each offset).

Accuracy of measured Be/B ratios in hambergite. Although the precision of the measurement is given above, the absolute ratio is unknown. However, the consistency between ratios measured at various energies and different polarities, coupled with the Be/B ion yield ratio given by two random phases (calculated relative to Ca) and the observations of Ottolini et al. (1993, 2002), would support a reasonable inference that the values given are accurate to < ±5%. The hambergite sample has, within error, a close-to-ideal Be/B ratio.

Single-crystal X-ray and neutron diffraction experiments

Two crystals optically free of defects and twinning (common in hambergite, e.g., Drugman and Goldschmidt 1912; Switzer et al. 1965; Richards 1996) were selected, under a transmitted-light polarizing microscope, for the diffraction experiments. The unit-cell parameters of our hambergite were measured by single-crystal X-ray diffraction using a KUMA diffractometer equipped with a point detector (crystal size: 0.35 × 0.280 × 0.080 mm^3). A total number of 42 reflections were centered giving a metrically orthorhombic lattice with: $a = 9.762(2)$, $b = 12.201(2)$, and $c = 4.430(1)$ Å [$V = 527.6(2)$ $Å^3$, Table 1].

Neutron Laue data were collected at room temperature from two rectangular single crystals (2.5 × 1.0 × 0.6 and 2.2 × 0.9 × 0.6 mm^3, Table 1) on the Laue diffractometer KOALA on the OPAL reactor at the Australian Nuclear Science and Technology Organisation. KOALA, which is essentially a clone of the Laue diffractometer VIVALDI at the Institut Laue-Langevin, Grenoble (McIntyre et al. 2006), uses the Laue diffraction technique on an unmonochromated thermal-neutron beam with a large solid-angle (8 sterad) cylindrical image-plate detector to increase the detected diffracted intensity by one-to-two orders of magnitude compared with a conventional monochromatic experiment. Each crystal was mounted with all face normals, and thence likely high-symmetry axes, well away from the single instrument rotation axis to avoid bias in the final refined anisotropic displacement parameters due to the blind region in reciprocal space around the rotation axis. Nine Laue diffraction patterns, each accumulated over 100 min on average, were collected at 10° or 20° intervals in rotation of the first crystal perpendicular to the incident neutron beam; a further 14 patterns were collected in the same manner from the second crystal. Typical Laue patterns from the two crystals are shown in Figure 2, where it can be seen that the second crystal is of better quality than the first. Nevertheless, the data from both crystals, which extended to a minimum d spacing of 0.54 Å for crystal 1 and 0.48 Å for crystal 2 were included in the analysis to ensure a better coverage of reciprocal space.

The Laue patterns were indexed using the program LAUEGEN of the Daresbury Laboratory Laue Suite (Campbell 1995; Campbell et al. 1998), and the reflections integrated using the program INTEGRATE+, which uses a two-dimensional version of the minimum σ(*I*)/*I* algorithm (Wilkinson et al. 1988). The individual re-

Table 1. Details of neutron data collection and refinement of hambergite

Crystal shape	Rectangular plate
Crystal size (mm^3)	2.5 × 1.0 × 0.6 (no. 1) 2.2 × 0.9 × 0.6 (no. 2)
Crystal color	Translucent white
Unit-cell constants	$a = 9.762(2)$ Å $b = 12.201(2)$ Å $c = 4.430(1)$ Å $V = 527.6(2)$ $Å^3$
Chemical formula	Be_2BO_3OH
Space group	*Pbca*
Z	8
T (K)	298
Radiation	Polychromatic, neutron
Diffractometer	KOALA, Laue diffractometer
$\lambda_{min}/\lambda_{max}$ (Å)	0.82/3.0
d_{min} (Å)	0.48
	$-17 \le h \le 17$
	$-25 \le k \le 24$
	$-9 \le l \le 6$
No. measured reflections	23236
No. unique reflections	1732
No. unique refl. with $F_o > 4\sigma(F_o)$	1430
No. refined parameters	76
R_{int}	0.0751
R_1 (F) with $F_o > 4\sigma(F_o)$	0.0504
R_1 (F) for all the unique reflections	0.0733
wR_2 (F^2)	0.0832
GooF	1.839
Weighting scheme: *a*, *b*	0.01, 0
Residuals (fm/$Å^3$)	+1.7/−3.0

Notes: $R_{int} = \Sigma|F^2_{obs} - F^2_{obs}(mean)|/\Sigma[F^2_{obs}]$; $R_1 = \Sigma||F_{obs}| - |F_{calc}||/\Sigma|F_{obs}|$; $wR_2 = \{\Sigma[w(F^2_{obs} - F^2_{calc})^2]/\Sigma[w(F^2_{obs})^2]\}^{0.5}$, $w = 1/[\sigma^2(F^2_{obs}) + (a \cdot P)^2 + b \cdot P]$, $P = [Max(F^2_{obs}, 0) + 2 \cdot F^2_{calc}]/3$. Unit-cell constants from the X-ray study (see text for details).

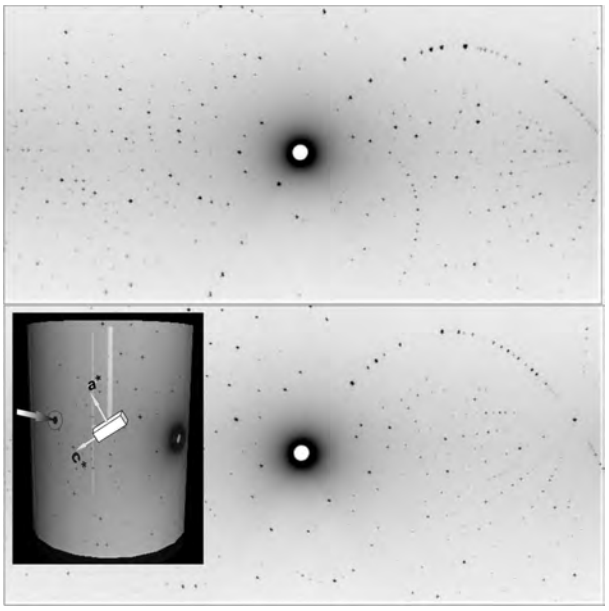

FIGURE 2. Typical neutron Laue patterns from the two crystals of hambergite (**above**: crystal 1, **below**: crystal 2). Each pattern subtends 8 sterad (288° horizontally × 104° vertically) at the sample and contains about 1450 Laue spots. The incident neutron beam exits the cylindrical image-plate detector through the central hole. The inset in the lower pattern shows the geometry of the cylindrical detector and the alignment for that pattern of crystal 2 to the incident neutron beam, which is depicted as an arrow at left. (The crystal volume is greatly exaggerated.)

flections were corrected for absorption using the calculated (wavelength-dependent) absorption coefficient, 0.675 λ + 0.032 mm^{-1} (transmission range: 0.212–0.745). The reflections were normalized for the incident wavelength, using a curve derived by comparing equivalent reflections and multiple observations, and corrected for the different angles of incidence via the local program LAUE4 (Piltz 2011). Reflections were observed with wavelengths between 0.74 and 5.2 Å, but only those with wavelengths between 0.82 and 3.0 Å were accepted for scaling, as reflections outside this range were too weak or had too few equivalents to be able to determine the normalization curve with confidence. In all 38 691 reflections were observed, of which 23 236 were single reflections with wavelengths between 0.82 and 3.0 Å, and yielded 1732 unique reflections in space group *Pbca* (Table 1).

Structure refinement

The intensity data of hambergite were first processed with the program E-STATISTICS, implemented in the WinGX package (Farrugia 1999), which calculates the normalized structure factors (E's) and their statistics of distributions. The structure of hambergite was found to be centrosymmetric at 77.3% likelihood. Accordingly, the Sheldrick $|E^2 - 1|$ criterion (Sheldrick 1997) indicated that the structure is centrosymmetric ($|E^2 - 1| = 0.914$). The anisotropic crystal-structure refinement was then performed in the space group *Pbca* using the SHELX-97 software (Sheldrick 2008), starting from the atomic coordinates of Burns et al. (1995), without any H site, and using the lattice parameters based on single-crystal X-ray diffraction (Table 1). The neutron scattering lengths of Be, B, O, F, and H have been used according to Sears (1986). Significant secondary isotropic extinction was evident in the initial refinements but was adequately corrected by Larson's formalism (1967), as implemented in the SHELXL-97 package. Convergence was rapidly achieved with one intense negative residual peak at $x \approx 0.314$, $y \approx 0.223$, $z \approx 0.458$ found in the final difference-Fourier map of the nuclear density (Fig. 3). Further cycles of refinement were then performed assigning H to these residual peaks, as hydrogen has a negative neutron scattering length. Convergence was rapidly achieved with all the principal mean-square atomic displacement parameters positively defined, including those for the H-site. The variance-covariance matrix showed no significant correlation among the refined parameters and at the end of the last cycle of refinement no peak larger than +1.7/–3.0 fm/$Å^3$ was

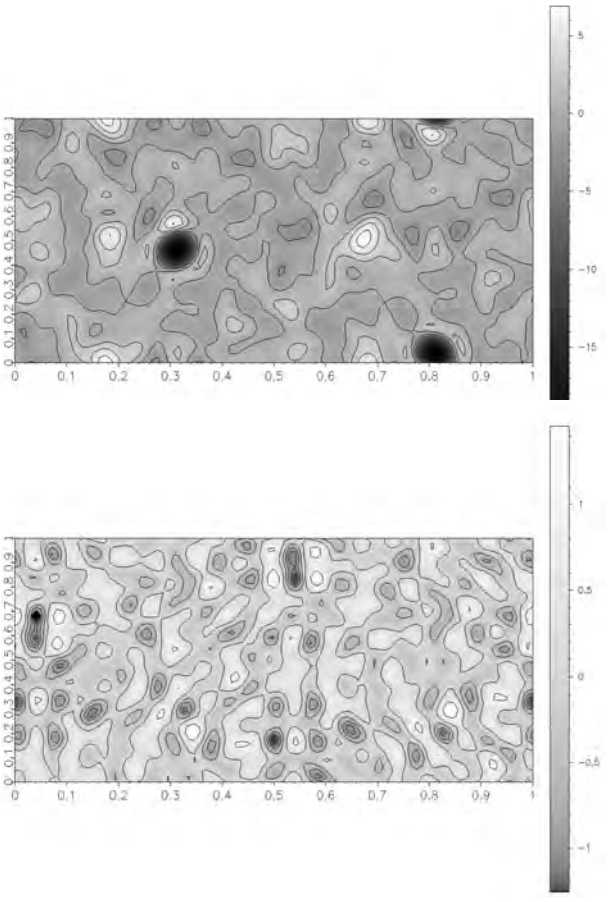

FIGURE 3. Difference Fourier maps of the nuclear density (fm/$Å^3$) of hambergite at y ~0.223 (**above**) after the first cycles of refinement without the H site, showing one intense negative residual peak at x ~0.314, z ~0.458, and (**below**) after the assignment of the H site. The grayscale is different for the two maps. Map orientation: $\overset{x}{\rightarrow}$.

present in the final difference-Fourier map of the nuclear density (Fig. 2, Table 1). The final agreement index (R_1) was 0.0504 for 76 refined parameters and 1430 unique reflections with $F_o > 4\sigma(F_o)$ (Table 1). Site coordinates and displacement parameters are reported in Tables 2 and 3. Bond lengths and angles are given in Table 4. A CIF[1] is deposited.

RESULTS AND DISCUSSION

The chemical analyses show that the composition of our hambergite sample is close the ideal one (i.e., Be_2BO_3OH) as only a low amount of F (i.e., 0.7–0.8 wt% by SIMS and EMPA-WDS, which corresponds to ~0.04 apfu), substituting the OH-group, occurs. The chemical analysis of hambergites from Anjanabonoina reported by Switzer et al. (1965) shows a F content ranging between 0.7–1 wt%, and a (Si+Al+Fe+Mg+Ca) content <0.01 wt%, in good agreement with our results. In addition, the unit-cell parameters measured by single-crystal X-ray diffraction in this study are consistent with an almost OH end-member hambergite

[1] Deposit item AM-12-086, CIF. Deposit items are available two ways: For a paper copy contact the Business Office of the Mineralogical Society of America (see inside front cover of recent issue) for price information. For an electronic copy visit the MSA web site at http://www.minsocam.org, go to the *American Mineralogist* Contents, find the table of contents for the specific volume/issue wanted, and then click on the deposit link there.

TABLE 2. Positional and anisotropic displacement parameters (Å²) of hambergite

Site	*x*	*y*	*z*	U_{eq}	U_{11}	U_{22}	U_{33}	U_{12}	U_{13}	U_{23}
Be1	0.00261(4)	0.18871(4)	0.26018(8)	0.00651(9)	0.0072(2)	0.0060(1)	0.0063(1)	0.0003(1)	–0.0002(1)	–0.00011(8)
Be2	0.23724(5)	0.06757(3)	0.27717(8)	0.00650(8)	0.0078(2)	0.0059(1)	0.0058(1)	0.0008(1)	0.0002(1)	–0.0001(1)
B	0.10617(6)	0.10704(4)	0.77298(10)	0.00451(10)	0.0046(1)	0.0041(2)	0.0041(2)	0.0015(2)	–0.0001(1)	0.0003(1)
O1	0.03760(6)	0.18766(4)	0.61914(10)	0.00697(9)	0.0101(2)	0.0056(1)	0.0052(2)	0.0026(1)	–0.0010(1)	–0.0002(1)
O2	0.10120(6)	0.10302(4)	0.08204(10)	0.00665(9)	0.0081(2)	0.0072(1)	0.0047(1)	0.0026(1)	–0.0002(1)	–0.0001(1)
O3	0.18691(6)	0.03450(4)	0.61701(10)	0.00731(9)	0.0100(2)	0.0068(1)	0.0051(2)	0.0039(1)	0.0009(1)	0.0009(1)
O4	0.33976(7)	0.17302(4)	0.29600(12)	0.00839(14)	0.0065(3)	0.0081(2)	0.0106(2)	–0.0017(2)	0.0011(2)	–0.0015(1)
H	0.3138(1)	0.2228(1)	0.4574(3)	0.0238(4)	0.0231(8)	0.0226(5)	0.0258(6)	–0.0015(5)	0.0060(4)	–0.0108(4)

Notes: The anisotropic displacement factor exponent takes the form: $-2\pi^2[(ha^*)^2U_{11} + \ldots + 2hka^*b^*U_{12}]$. U_{eq} is defined as one third of the trace of the orthogonalized U_{ij} tensor. The site occupancy factor (s.o.f.) of O4 and H is not constrained to 100%, the following refined s.o.f are obtained: 98.0(4)% for O4 and 95.4(9)% for H, respectively.

TABLE 3. Principal root-mean-square components (R1, R2, and R3, ×10² Å) of the atomic displacements parameters

Site	R1	R2	R3	R1/R3
Be1	8.5(1)	7.87(6)	7.68(6)	1.11
Be2	9.0(1)	7.62(6)	7.48(7)	1.20
B	7.9(1)	6.4(1)	5.6(2)	1.43
O1	10.68(9)	7.14(7)	6.6(1)	1.61
O2	10.10(9)	7.1(1)	6.86(7)	1.47
O3	11.31(9)	7.1(1)	6.4(1)	1.77
O4	10.91(9)	8.9(1)	7.3(2)	1.48
H	19.3(1)	14.7(2)	11.2(3)	1.73

following Burns et al. (1995), as the F↔OH substitution causes a significant change of the unit-cell dimensions.

The neutron structure refinement confirmed the general structure model of hambergite previously described by means of X-ray diffraction (e.g., Zachariasen 1931; Zachariasen et al. 1963; Burns et al. 1995). A general view of the crystal structure of hambergite, based on the anisotropic refinements of this study, is shown in Figure 1. The Be sites appear to be fully occupied by beryllium and the B site fully occupied by boron. The two Be tetrahedra appear to be significantly distorted, as the differences between the longest and the shortest bond lengths (Δ_{max}) are: Δ_{max}(Be1) ≈ 0.048 Å and Δ_{max}(Be2) ≈ 0.029 Å (Table 4). In contrast, the BO_3 group shows an almost ideal triangular configuration, with Δ_{max}(B) ≈ 0.001 Å and <O-B-O> ≈ 120.0° (Table 4). A similar experimental finding has been reported by Burns et al. (1995) on the basis of X-ray structure refinements.

The analysis of the nuclear-density Fourier maps shows that in our hambergite sample only one independent H site is present. A refinement conducted with unconstrained site occupancy led to a refined occupancy factor of 95.4(9)% (Table 2). The use of F and O neutron scattering lengths to model the occupancy of the O4 site did not allow the refinement of the F/O fraction, not surprising in view of the low-F content and for the similar F/O scattering lengths (i.e., 5.805 fm for O and 5.654 fm for F). A refinement conducted with the scattering length of oxygen alone at the O4 site and unconstrained site occupancy led to a refined occupancy factor of 98.0(4)% (Table 2), suggesting the presence of F. These results are in good agreement with the experimental findings based on SIMS and EMPA-WDS [i.e., chemical analyses: $Be_2BO_3(OH_{0.96}F_{0.04})$; structure refinement: $Be_2BO_3(OH_{0.95}F_{0.05})$].

The geometry of the hydroxyl group and hydrogen bonding in hambergite is now well defined: only one independent H site was located and the O4-H distance, corrected for "riding motion" (Busing and Levy 1964), is ~0.9929 Å (Table 4). Four possible hydrogen bonds have been found (all with O···O < 3.3 Å, Table 4) but only one appears to be energetically favorable with O4 as *acceptor*, and with O4···O4 = 2.904(1) Å, H···O4 = 1.983(1) Å, and O4-H···O4 = 157.5(1)° (Table 4). In other words, O4 acts as *donor* and as *acceptor* of the hydrogen bond, with a zigzag chain of H-bonds along [001] (Fig. 1). The deviation of the O4-H···O4 bond from linearity is likely due to the H-Be1 repulsion, as the distance H-Be1 is significantly short (i.e., ~2.12 Å) with O4-H···O4 ~157.5° and would be shorter if the O4-H···O4 angle were 180°. The configuration of the hydrogen bonding in the hambergite structure is shown in Figure 1.

Burns et al. (1995) showed how the substitution of F at the O4 site leads to the loss of O4-H···O4 bond with a consequent "distortion" of the structure, resulting in a significant increase of the unit-cell edge along [010] with an expansion of the O4···O4 dis-

TABLE 4. Relevant bond distances (Å) and angles (°) in the hambergite structure

	Uncorrected distance	Riding motion	Non-correlated motion	Rigid-body motion
Be1-O1	1.6265(7)			1.6269
Be1-O1′	1.6680(7)			1.6684
Be1-O2	1.6255(7)			1.6256
Be1-O4	1.6204(8)			1.6221
<Be1-O>	1.6351			1.6357
Be2-O2	1.6426(7)			1.6427
Be2-O3	1.6342(7)			1.6349
Be2-O3′	1.6132(6)			1.6139
Be2-O4	1.6321(7)			1.6338
<Be2-O>	1.6305			1.6313
B-O1	1.3712(7)	1.3734	1.3809	
B-O2	1.3709(7)	1.3732	1.3806	
B-O3	1.3719(7)	1.3745	1.3818	
<B-O>	1.3713	1.3737	1.3811	
O4-H	0.9714(14)	0.9929	1.0105	
O4···O1	3.284(1)			
H···O1	2.822(2)			
O4-H···O1	110.0(1)			
O4···O1	2.600(1)			
H···O1	2.467(2)			
O4-H···O1	86.8(1)			
O4···O1	3.236(1)			
H···O1	2.911(2)			
O4-H···O1	100.8(1)			
O4···O4	2.904(1)			
H···O4	1.983(1)			
O4-H···O4	157.5(1)			
O1-Be1-O1	109.29(3)		O2-Be2-O3	107.86(4)
O1-Be1-O2	110.19(4)		O2-Be2-O3	110.65(3)
O1-Be1-O4	110.81(4)		O2-Be2-O4	108.36(4)
O1-Be1-O2	106.18(3)		O3-Be2-O3	110.65(3)
O1-Be1-O4	104.49(4)		O3-Be2-O4	109.38(3)
O2-Be1-O4	115.49(4)		O3-Be2-O4	110.47(4)
O1-B-O2	120.32(5)			
O1-B-O3	119.54(4)			
O2-B-O3	120.02(5)			

Note: Bond distance corrected for "riding motion" and "non-correlated motion" following Busing and Levy (1964); bond distances corrected for "rigid body motions" following Downs et al. (1992) and Downs (2000).

tance (i.e., donor-acceptor distance) in response to the increased F content. For almost ideal Be_2BO_3OH hambergite, the O4···O4 distance was found to be ~2.90 Å, in good agreement with the experimental findings of this study (i.e., chemical composition and structure refinement, Table 4).

Our data confirm the pleochroic scheme of the infrared spectra of hambergite by Vergnoux and Ginouvès (1955): a significant pleochroism of the two distinct bands in the stretching region of the hydroxyl group occurs, with the highest absorption with *E*//[001] and the lowest absorption with *E*//[100]. Vergnoux and Ginouvès (1955) suggested that the O-H bond has a strong component of vibration parallel to the **c** axis. Our structure refinement shows that the angle between the O-H bond direction and [001] is ~15°, the angle between O-H and [100] is ~75°, and the angle between O-H and [010] is ~39°. The unpolarized infrared spectra of two hambergites from Anjanabonoina, Madagascar (RRUFF ID: R050672), and Momeik, Burma (RRUFF ID: R050603), available in the RRUFF database (http://rruff.info, Downs 2006) both show two intensive modes, ascribable to stretching vibrations of the hydroxyl group, at 3415 and 3520 cm^{-1}, respectively. The two modes suggest at least two distinct hydrogen-bonding environments, with "weak" (sensu Libowitzky and Beran 2006) or "moderate" (sensu Gilli and Gilli 2009) H-bonds. Within the resolution limit of our structure refinement, we found only one independent proton site, and the magnitude of its anisotropic displacement regime does not suggest site splitting (Table 3). However, for the *donor* site (i.e., O4), we observed: (1) F/O disorder at a local scale and (2) a different bond strength with Be1 and Be2, as Be1-O4 (~1.620 Å, Table 4) and Be2-O4 (~1.632 Å, Table 4). It is highly likely that the two absorption bands reflect the F ↔ O substitution, leading to two different hydrogen-bonding environments (i.e., $O4\text{-}H\cdots O_{O4site}$ and $O4\text{-}H\cdots F_{O4site}$), and the different bonding regime of O4 shared by two tetrahedra. We dismiss the possibility that the two absorption bands in the OH stretching region are due to H-bonds with O1 as acceptor: despite all the three independent O4···O1 being <3.3 Å (Table 4), the "compressed" O4-H···O1 angles (~110°, ~101°, and ~87°, respectively, Table 4) appear to be non-realistic for H-bonds. The two bands ascribable to two H-bond environments with O4 as *donor* and $(O,F)_{O4}$ as *acceptors* agree well with the correlation function of O-H infrared stretching frequencies and O···O/F hydrogen bond lengths of Libowitzky (1999) and Libowitzky and Beran (2006).

This study illustrates several advantages offered by modern neutron Laue diffraction for structural determination of natural mineral samples. First and foremost is that comparatively small single crystals can be used (0.1 to 1 mm^3 is the norm), necessary in this particular study because of the large absorption of neutrons by natural boron. The easy visualization of the projection of the extensive volume of reciprocal space observed in one Laue pattern allows rapid verification that the crystal is single phase. The Laue technique does require good quality single crystals, but this is easier to satisfy given the small volumes acceptable.

Acknowledgments

The authors thank the Bragg Institute, Australian Nuclear Science and Technology Organisation, for the allocation of neutron beam time. Two anonymous reviewers, the Associate Editor (S. Redfern) and the Technical Editor (R. Peterson) are thanked. The authors thank C. de Hoog (IMF, Edinburgh) for his assistance with the SIMS analysis and NERC for supporting access to equipment.

References cited

Brögger, W.C. (1890) Die Mineralien der Syenitpegmatitgänze der südnorwegischen Augit-und Nephelinsyenite. Zeitschrift für Kristallographie, Mineralogie und Petrographie, 16, 65–67.

Burns, P.C., Novák, M., and Hawthorne, F.C. (1995) Fluorine-hydroxyl variation in hambergite: a crystal-structure study. Canadian Mineralogist, 33, 1205–1213.

Busing, W.R. and Levy, H.A. (1964) The effect of thermal motion on the estimation of bond lengths from diffraction measurements. Acta Crystallographica, 17, 142–146.

Campbell, J.W. (1995) LAUEGEN, an X-windows-based program for the processing of Laue diffraction data. Journal of Applied Crystallography, 28, 228–236.

Campbell, J.W., Hao, Q., Harding, M.M., Nguti, N.D., and Wilkinson, C. (1998) LAUEGEN version 6.0 and INTLDM. Journal of Applied Crystallography, 31, 496–502.

Černý, P. and Ercit, T.S. (2005) The classification of granitic pegmatites revisited. Canadian Mineralogist, 43, 2005–2026.

De Vito, C., Pezzotta, F., Ferrini, V., and Aurisicchio, C. (2006) Nb-Ti-Ta oxides in the Anjanabonoina pegmatite, central Madagascar: a record of magmatic and post-magmatic events. Canadian Mineralogist, 44, 87–103.

Dirlam, D.M., Laurs, B.M., Pezzotta, F., and Simmons, W.B. (2002) Liddicoatite tourmaline from Anjanabonoina, Madagascar. Gems and Gemology, 38, 28–52.

Downs, R.T. (2000) Analysis of harmonic displacement factors. In R.M. Hazen and R.T. Downs, Eds., High-Temperature and High-Pressure Crystal Chemistry, vol. 41, p. 61–117. Reviews in Mineralogy and Geochemistry, Mineralogical Society of America and Geochemical Society, Chantilly, Virginia, U.S.A.

——— (2006) The RRUFF Project: an integrated study of the chemistry, crystallography, Raman and infrared spectroscopy of minerals (http://rruff.info/). Program and Abstracts of the 19th General Meeting of the International Mineralogical Association in Kobe, Japan, O03-13.

Downs, R.T., Gibbs, G.V., Bartelmehs, K.L., and Boisen, M.B. Jr. (1992) Variations of bond lengths and volumes of silicate tetrahedra with temperature. American Mineralogist, 77, 751–757.

Drugman, J. and Goldschmidt, V. (1912) Ein Hambergitzwilling von Madagascar. Zeitschrift für Kristallographie, Mineralogie und Petrographie, 50, 596–597.

Farrugia, L.J. (1999) WinGX suite for small-molecule single-crystal crystallography. Journal of Applied Crystallography, 32, 837–838.

Fernandez, A., Huber, S., Schreurs, G., Villa, I., and Rakotondrazafy, M. (2001) Tectonic evolution of the Itremo region (central Madagascar) and implications for Gondwana assembly. Gondwana Research, 4, 165–168.

Gatta, G.D., Nestola, F., Bromiley, G.D., and Mattauch, S. (2006) The real topological configuration of the extra-framework content in alkali-poor beryl: a multi-methodological study. American Mineralogist, 91, 29–34.

Gatta, G.D., Rotiroti, N., McIntyre, G.J., Guastoni, A., and Nestola, F. (2008) New insights into the crystal chemistry of epididymite and eudidymite from Malosa, Malawi: a single-crystal neutron diffraction study. American Mineralogist, 93, 1158–1165.

Gatta, G.D., Vignola, P., McIntyre, G.J., and Diella, V. (2010) On the crystal chemistry of londonite $[(Cs,K,Rb)Al_4Be_5B_{11}O_{28}]$: a single-crystal neutron diffraction study at 300 and 20 K. American Mineralogist, 95, 1467–1472.

Gilli, G. and Gilli, P. (2009) The Nature of Hydrogen Bond. International Union of Crystallography Monographs on Crystallography, vol. 23, Oxford Science Publication, 336 p.

Larson, A.C. (1967) Inclusion of secondary extinction in least-squares calculations. Acta Crystallographica, 23, 664–665.

Libowitzky, E. (1999) Correlation of O-H stretching frequencies and O-H···O hydrogen bond lengths in minerals. Monatshefte für Chemie, 130, 1047–1059.

Libowitzky, E. and Beran, A. (2006) The structure of hydrous species in nominally anhydrous minerals: Information from polarized IR spectroscopy. In H. Keppler and J.R. Smyth, Eds., Water in Nominally Anhydrous Minerals, vol. 62, p. 29–52. Reviews in Mineralogy and Geochemistry, Mineralogical Society of America and Geochemical Society, Chantilly, Virginia, U.S.A.

McIntyre, G.J., Lemée-Cailleau, M.-H., and Wilkinson, C. (2006) High-Speed Neutron Laue Diffraction Comes of Age. Physica B, 385–386, 1055–1058.

Novák, M., Burns, P.C., and Morgan, G.B. VI (1998) Fluorine variation in hambergite from granitic pegmatites. Canadian Mineralogist, 36, 441–446.

Ottolini, L., Bottazzi, P., and Vannucci, R. (1993) Quantification of lithium, beryllium, and boron in silicates by secondary-ion mass spectrometry using conventional energy filtering. Analytical Chemistry, 65, 1960–1968.

Ottolini, L., Cámara, F., Hawthorne, F.C., and Stirling, J. (2002) SIMS matrix effects in the analysis of light elements in silicate minerals: Comparison with SREF and EMPA data. American Mineralogist, 87, 1477–1485.

Pezzotta, F. (1996) Preliminary data on the physical-chemical evolution of the gem-bearing Anjanabonoina pegmatite, central Madagascar. Proceedings of the Joint Meeting of the Geological Association of Canada and the Mineralogical Association of Canada, Winnipeg, Manitoba, May 27–29, A-75.

Pezzotta, F. (2001) Madagascar: A Mineral and Gemstone Paradise. Extralapis English, No. 1. Lapis International, LLC, East Hampton, CT, USA, 97 p.
Piltz, R.O. (2011) Accurate data analysis for the Koala and VIVALDI neutron Laue diffractometers. Abstracts of the XXII IUCr Congress, Madrid (Spain) 22–30 August 2011. Acta Crystallographica, A67, C155.
Richards, R.P. (1996) Twinned hambergite from the Gilgit district, Northern Pakistan. Canadian Mineralogist, 34, 615–621.
Sears, V.F. (1986) Neutron scattering lengths and cross-sections. In K. Sköld and D.L. Price, Eds., Neutron Scattering, Methods of Experimental Physics, vol. 23A, p. 521–550. Academic Press, New York.
Sheldrick, G.M. (1997) SHELX-97. Programs for crystal structure determination and refinement. University of Göttingen, Germany.
——— (2008) A short history of *SHELX*. Acta Crystallographica, A64, 112–122.
Switzer, G., Clarke, R.S., Sinkankas, J. Jr., and Worthing H.W. (1965) Fluorine in hambergite. American Mineralogist, 50, 85–95.
Vergnoux, A.M. and Ginouvès, M.F. (1955) Étude d'un cristal d'hambergite dans le proche infra-rouge. Nuovo Cimento, 2, 807–815.
Wilkinson, C., Khamis, H.W., Stansfield., R.F.D., and McIntyre, G.J. (1988) Integration of single-crystal reflections using area multidetectors. Journal of Applied Crystallography, 21, 471–478.
Zachariasen, W.H. (1931) The crystalline structure of hambergite, $Be_2BO_3(OH)$. Zeitschrift für Kristallographie, Mineralogie und Petrographie, 76, 289–302.
——— (1934) The crystal lattice of boric acid, BO_3H_3. Zeitschrift für Kristallographie, Mineralogie und Petrographie, 88, 150–161.
Zachariasen, W.H., Plettinger, H.A., and Marezio, M. (1963) The structure and birefringence of hambergite, $Be_2BO_3(OH)$. Acta Crystallographica, 16, 1144–1146.

Manuscript received May 17, 2012
Manuscript accepted July 23, 2012
Manuscript handled by Simon Redfern